Supporting Information

Electron-Beam Irradiation Enables Concurrent Thermoelectric and Mechanical Enhancement in Commercial *p*-Type $Bi_{0.5}Sb_{1.5}Te_3$

Fang Xu [a], Bo Liu [a], Kun Zhang [a,*], Ran Ang [a,b,c,*]

[a] *Key Laboratory of Radiation Physics and Technology, Ministry of Education, Institute of Nuclear Science and Technology, Sichuan University, Chengdu 610064, China*

[b] *College of Physics, Sichuan University, Chengdu 610064, China*

[c] *Institute of New Energy and Low-Carbon Technology, Sichuan University, Chengdu 610065, China*

** Corresponding author and Email: rang@scu.edu.cn) or kzhang@scu.edu.cn*

Theoretical Calculation.

The thermoelectric transport properties with the Single Parabolic Band (SPB) framework were calculated using standard expressions:[1]

Lorentz number (L):

$$L = \frac{k_B^2 3F_0F_2 - 4F_1^2}{e^2F_0^2} \tag{S1}$$

Seebeck coefficient (S):

$$S = \frac{k_B}{e}\left[\frac{\left(r+5/2\right)F_r + 3/2(\eta)}{\left(r+3/2\right)F_r + 1/2(\eta)} - \eta\right] \tag{S2}$$

Fermi Energy (F_j):

$$F_j(\eta) = \int_0^\infty \frac{\xi^j d\xi}{1+e^{(\xi-\eta)}} \tag{S3}$$

Effective mass (m^*):

$$m^* = \frac{h^2}{2k_BT}\left(\frac{n}{4\pi F_{1/2}(\mu)}\right)^{\frac{2}{3}} \tag{S4}$$

Here, k_B denotes the Boltzmann constant, e represents the electron charge, r indicates the scattering factor, η signifies the bonding potential, h stands for Planck's constant, and T represents the absolute temperature.

The weighted mobility (μ_W) is given by the following expression:[2]

$$\mu_W = \frac{331}{\rho}\left(\frac{T}{300}\right)^{-\frac{3}{2}}\left[\frac{\exp\left(\frac{|S|}{k_B/e}-2\right)}{1+\exp\left[-5\left(\frac{|S|}{k_B/e}-1\right)\right]} + \frac{\frac{3|S|}{\pi^2 k_B/e}}{1+\exp\left[5\left(\frac{|S|}{k_B/e}-1\right)\right]}\right] \tag{S5}$$

To compare thermoelectric performance across finite temperature intervals, the average power factor (PF_{ave}) and average ZT_{ave} are defined as:

$$PF_{avg} = \frac{\int_{T_c}^{T_h} PF\,dT}{T_h - T_c} \tag{S6}$$

$$ZT_{avg} = \frac{\int_{T_c}^{T_h} ZT\,dT}{T_h - T_c} \tag{S7}$$

For the *p*-type $Bi_{0.5}Sb_{1.5}Te_3$ alloy studied here, bipolar diffusion becomes significant only above ~375 K. Therefore, at low temperatures (300-350 K), $\kappa_{ph} + \kappa_b \approx \kappa_{ph}$. The lattice thermal conductivity (κ_{ph}) in this range was fitted to the empirical form: $\kappa_{ph} = aT^{-1} + b$,[3] where a and b are fitting parameters (**Table** S2). This fit was extrapolated up to 503 K to estimate the full-range lattice contribution (κ_{ph}) and the calculated electronic thermal conductivity (κ_{ele}) from the experimentally measured total thermal conductivity (κ_{tot}).

Table S1. Elemental composition of *p*-type $Bi_{0.5}Sb_{1.5}Te_3$ samples obtained from EDS analysis of the regions shown in Figure. 3, before and after electron-beam irradiation.

Samples Name (*p*-type $Bi_{0.5}Sb_{1.5}Te_3$)	Bi (at%)	Sb (at%)	Te (at%)
Pristine	8.7	32.6	58.7
100 kGy	8.6	32.5	58.9
400 kGy	8.9	32.2	58.9
700 kGy	9.1	32.1	58.8
1000 kGy	8.6	32.3	59.1

Table S2. Fitting parameters (a and b) for the lattice thermal conductivity (κ_{ph}) of commercial p-type $Bi_{0.5}Sb_{1.5}Te_3$ samples (pristine, 100, 400, 700, and 1000 kGy) over 303-503 K, using the relation $\kappa_{ph} = aT^{-1}+b$.

	p-$Bi_{0.5}Sb_{1.5}Te_3$ Sample Designation				
	Pristine	100 kGy	400 kGy	700 kGy	1000 kGy
a	50.04	16.21	14.15	17.62	12.46
b	0.46	0.52	0.438	0.53	0.49

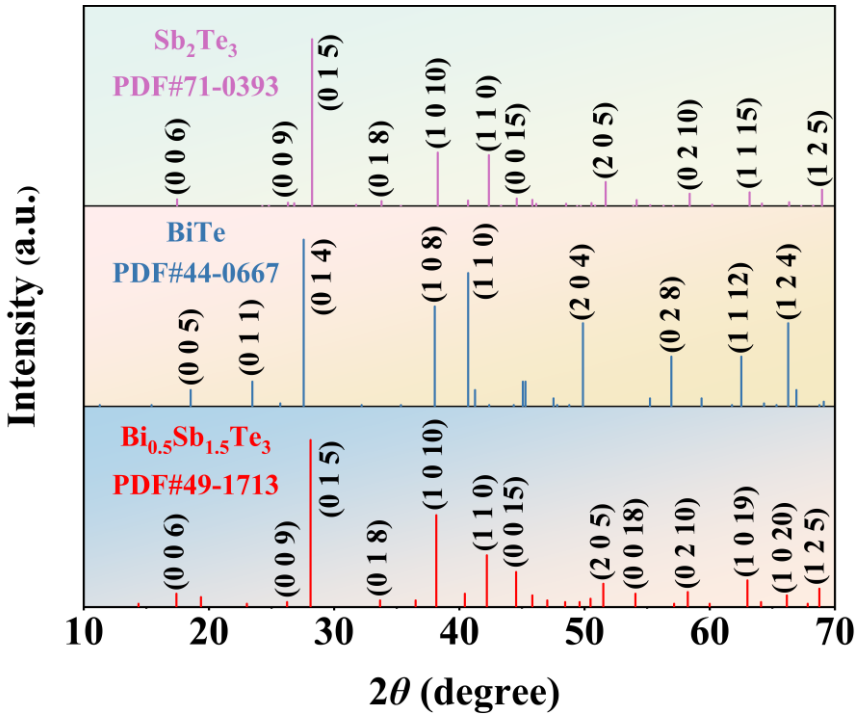

Fig. S1. Reference Powder Diffraction File (PDF) cards for the constituent phases: Sb_2Te_3, BiTe, and the $Bi_{0.5}Sb_{1.5}Te_3$ alloy used in this study.

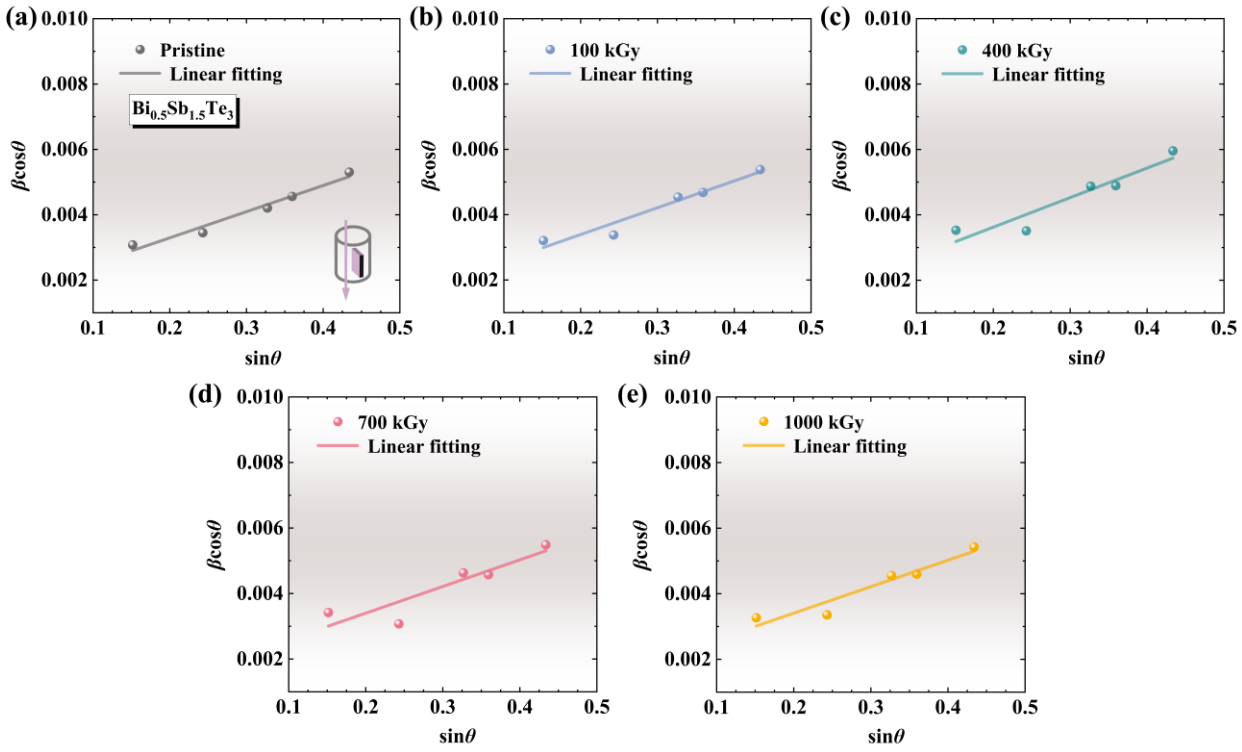

Fig. S2. Williamson-Hall plots of $\beta\cos\theta$ versus $\sin\theta$ for the commercially available *p*-type $Bi_{0.5}Sb_{1.5}Te_3$ samples, used to evaluate lattice microstrain and crystallite size.

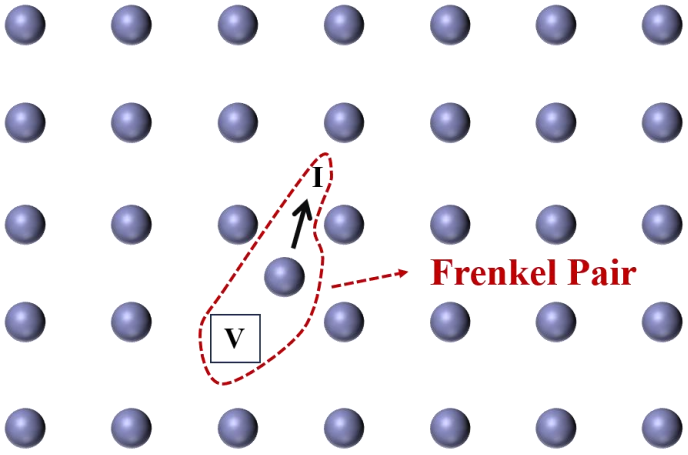

Fig. S3. Schematic illustration of vacancy-interstitial (Frenkel) pairs in the crystal lattice of *p*-type $Bi_{0.5}Sb_{1.5}Te_3$.

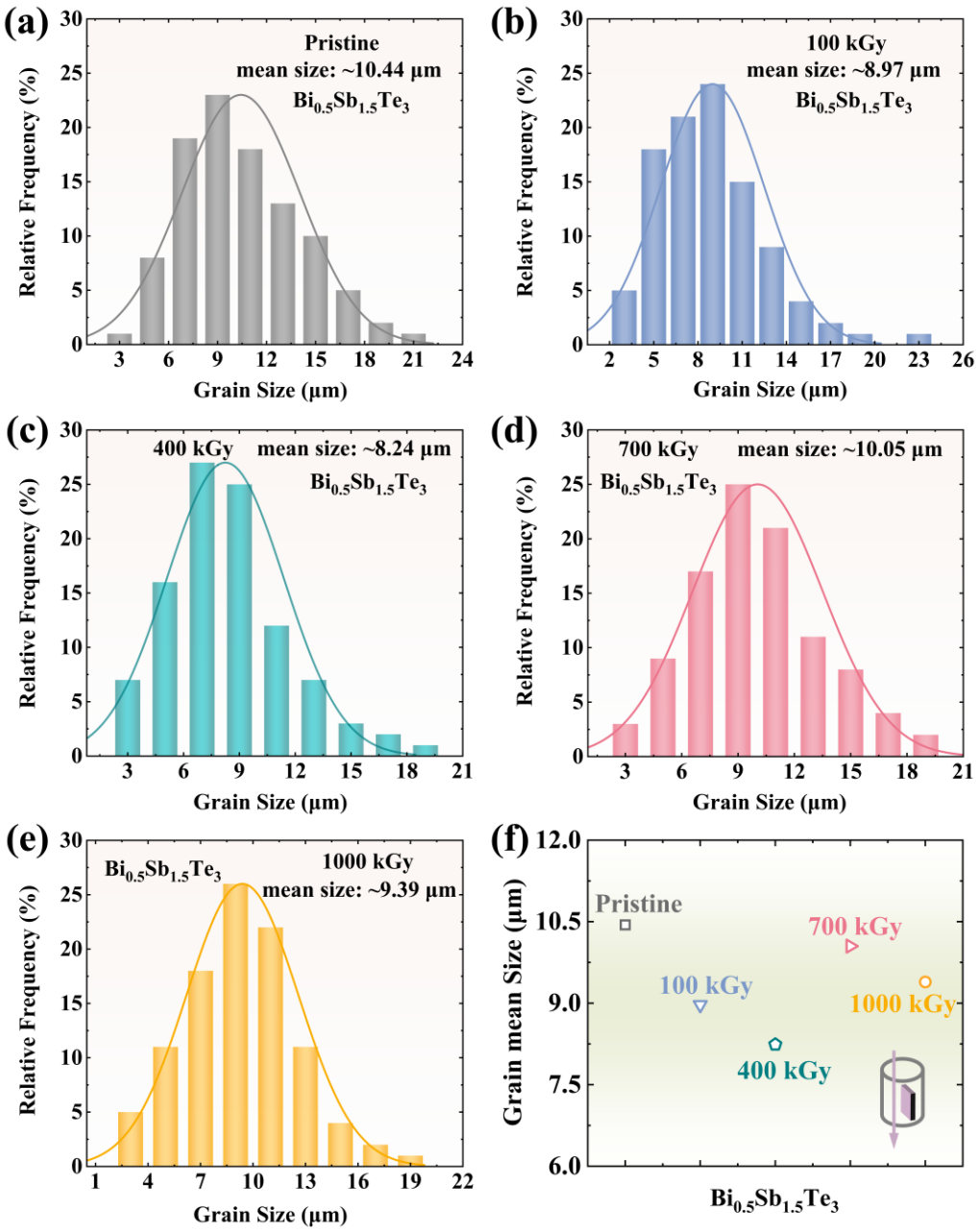

Fig. S4. Statistical analysis of grain size from fracture surfaces of *p*-type $Bi_{0.5}Sb_{1.5}Te_3$ before and after electron-beam irradiation. Panels (a)-(e) correspond to the pristine, 100, 400, 700, and 1000 kGy samples, respectively, consistent with the SEM images shown in Figure. 3. Panel (f) compares the grain size distributions extracted from (a)-(e). The inset indicates that the fracture surfaces are parallel to the hot-pressing direction.

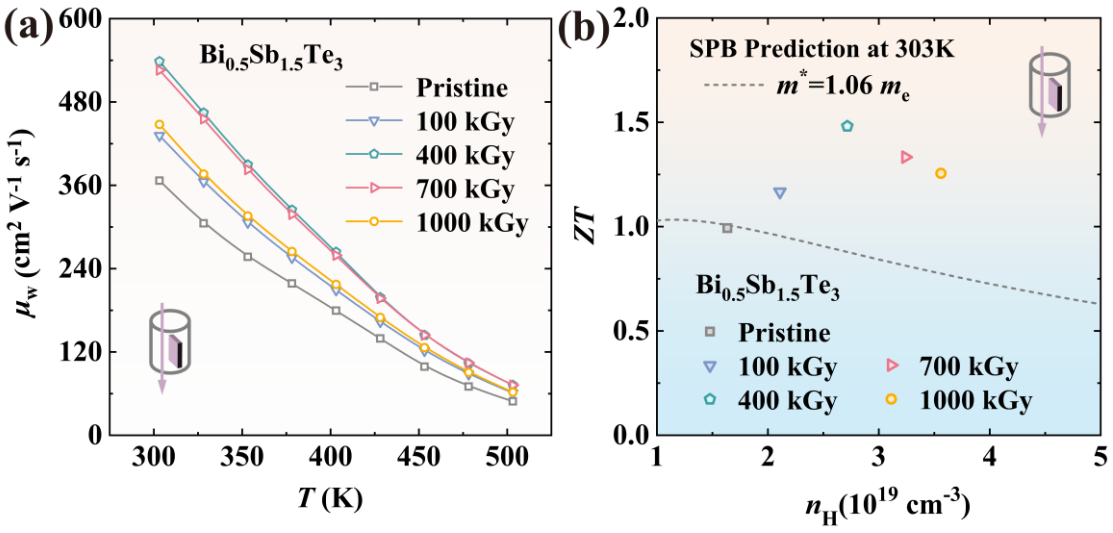

Fig. S5. (a) Temperature dependence of the weight mobility (μ_W) for *p*-type $Bi_{0.5}Sb_{1.5}Te_3$ samples: pristine, 100, 400, 700, and 1000 kGy. (b) Room-temperature *ZT* as a function of carrier concentration (n_H), analyzed using the single parabolic band (SPB) model.

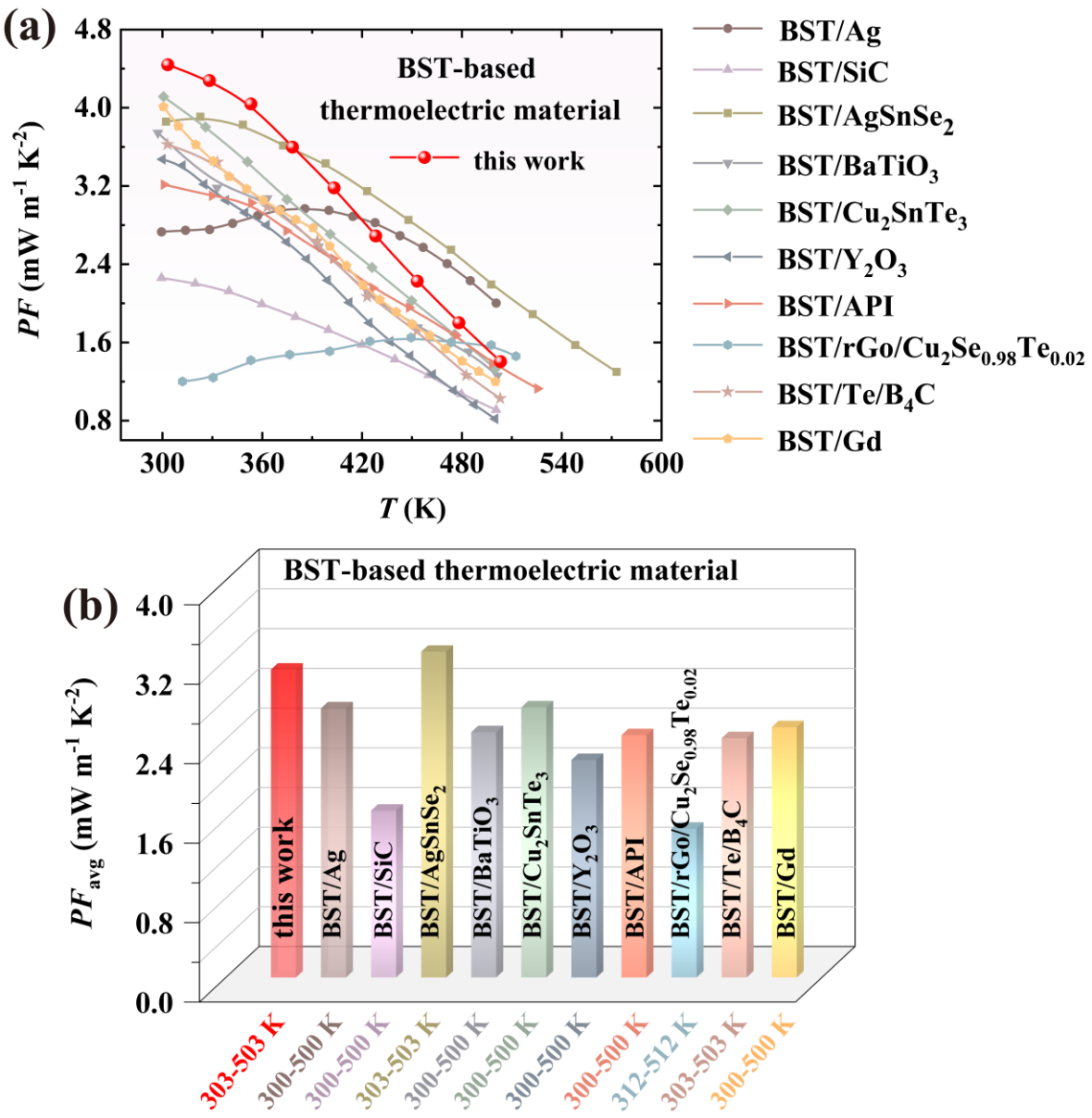

Fig. S6. Literature-reported power factor of BST-based optimized via interfacial engineering. (a) Temperature-dependent *PF*. (b) Average PF_{avg} over 303-503 K temperature range. References[4-13] correspond to previous studies employing various interface engineering strategies.

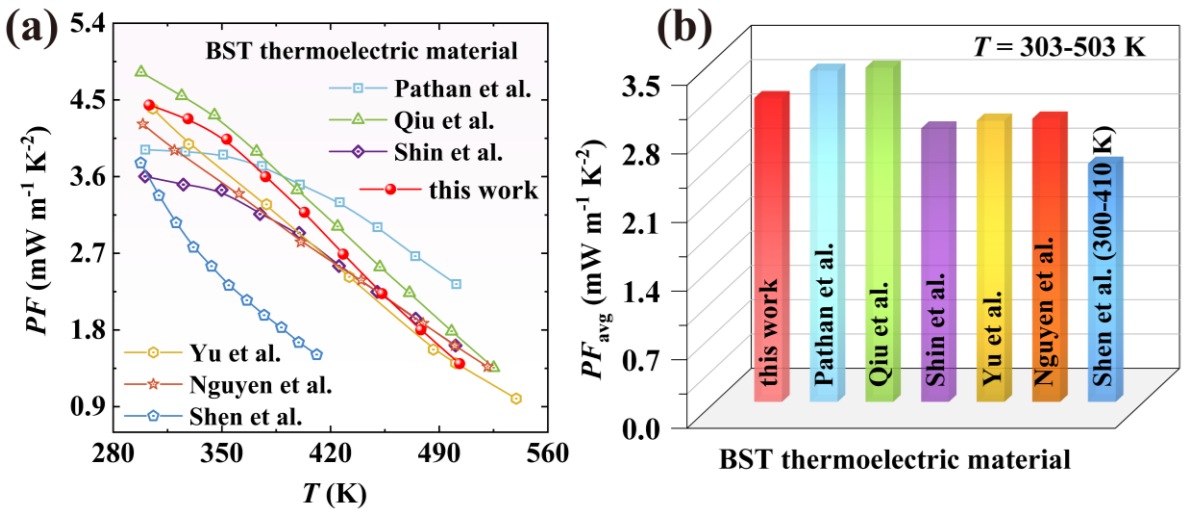

Fig. S7. Literature summary of *p*-type $Bi_{0.5}Sb_{1.5}Te_3$ optimized via various processing strategies.[14-19] (a) Temperature-dependent *PF*. (b) PF_{avg} over 303-503 K temperature range.

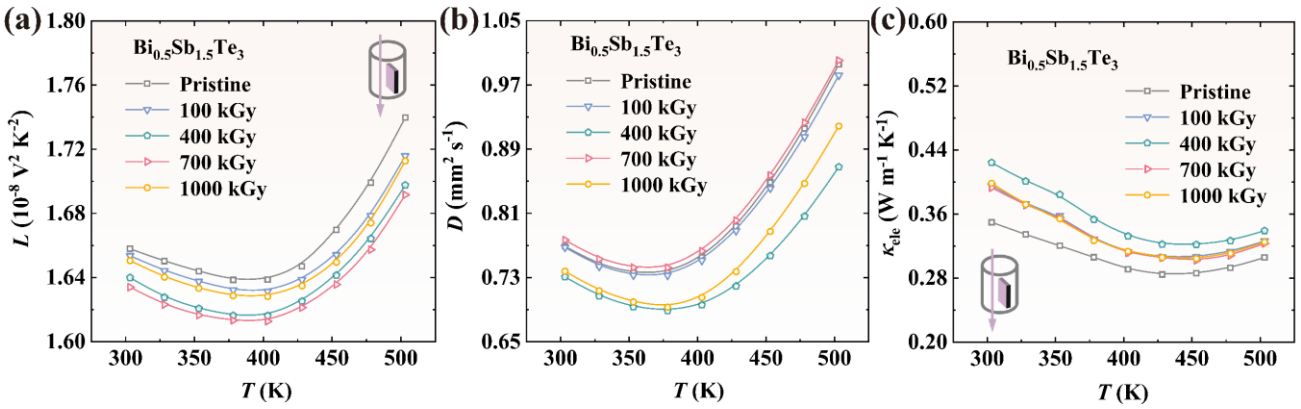

Fig. S8. Temperature dependence of key transport parameters for commercial *p*-type $Bi_{0.5}Sb_{1.5}Te_3$ samples (pristine, 100, 400, 700, and 1000 kGy) before and after electron-beam irradiation: (a) Lorentz number (*L*), (b) thermal diffusion coefficient (*D*), and (c) electronic thermal conductivity (κ_{ele}).

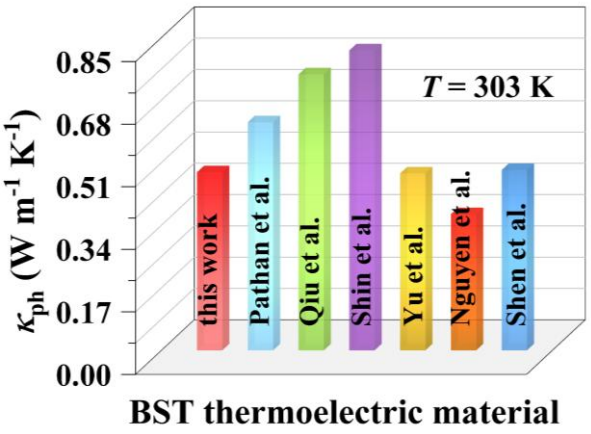

Fig. S9. Summary of reported room-temperature lattice thermal conductivity (κ_{ph}) for *p*-type $Bi_{0.5}Sb_{1.5}Te_3$ prepared via various optimized processing routes.[14-19]

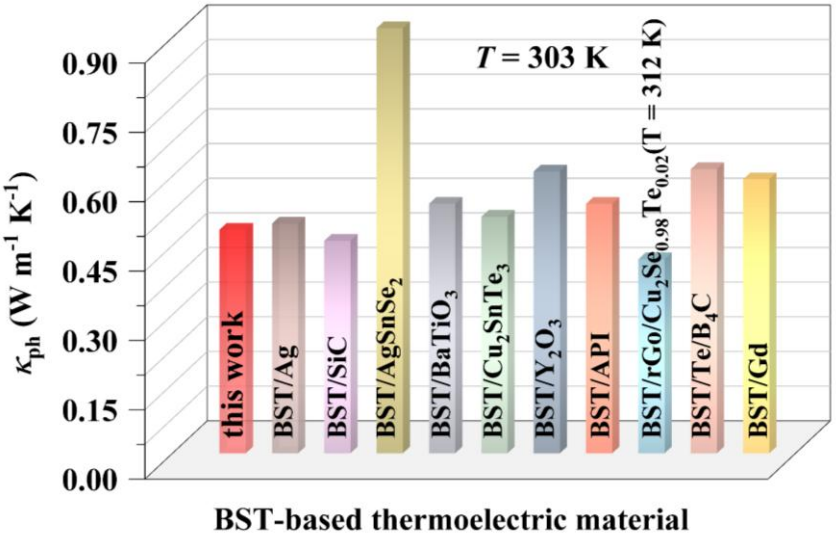

Fig. S10. Summary of reported room-temperature κ_{ph} for *p*-type $Bi_{0.5}Sb_{1.5}Te_3$/secondary phase composites.[4-13]

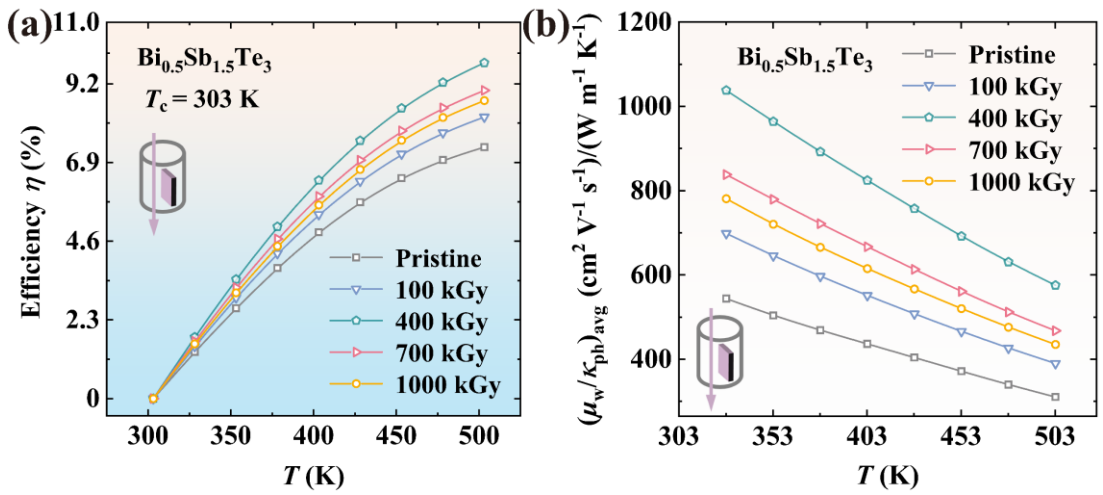

Fig. S11. Temperature-dependent theoretical thermoelectric conversion efficiency (η) and weighted mobility to lattice thermal conductivity ratio (μ_w/κ_{ph}) for commercial *p*-type $Bi_{0.5}Sb_{1.5}Te_3$ samples before and after electron-beam irradiation.

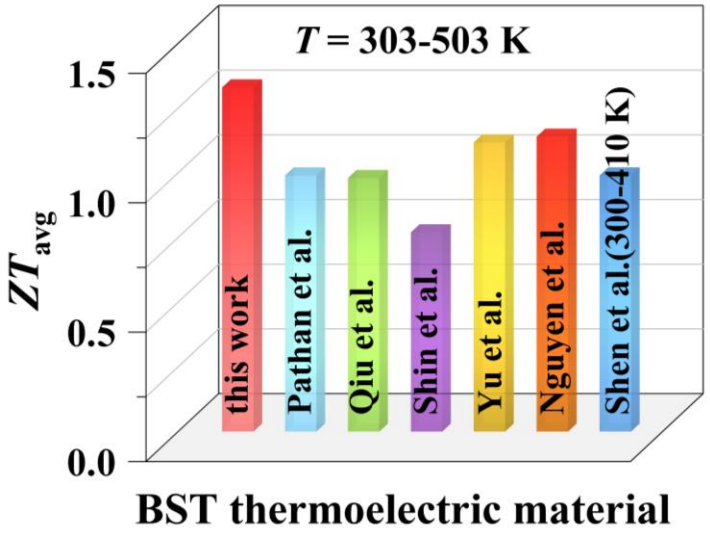

Fig. S12. Summary of reported average ZT_{avg} over 303-503 K for *p*-type $Bi_{0.5}Sb_{1.5}Te_3$ prepared via various optimized processing techniques.[14-19]

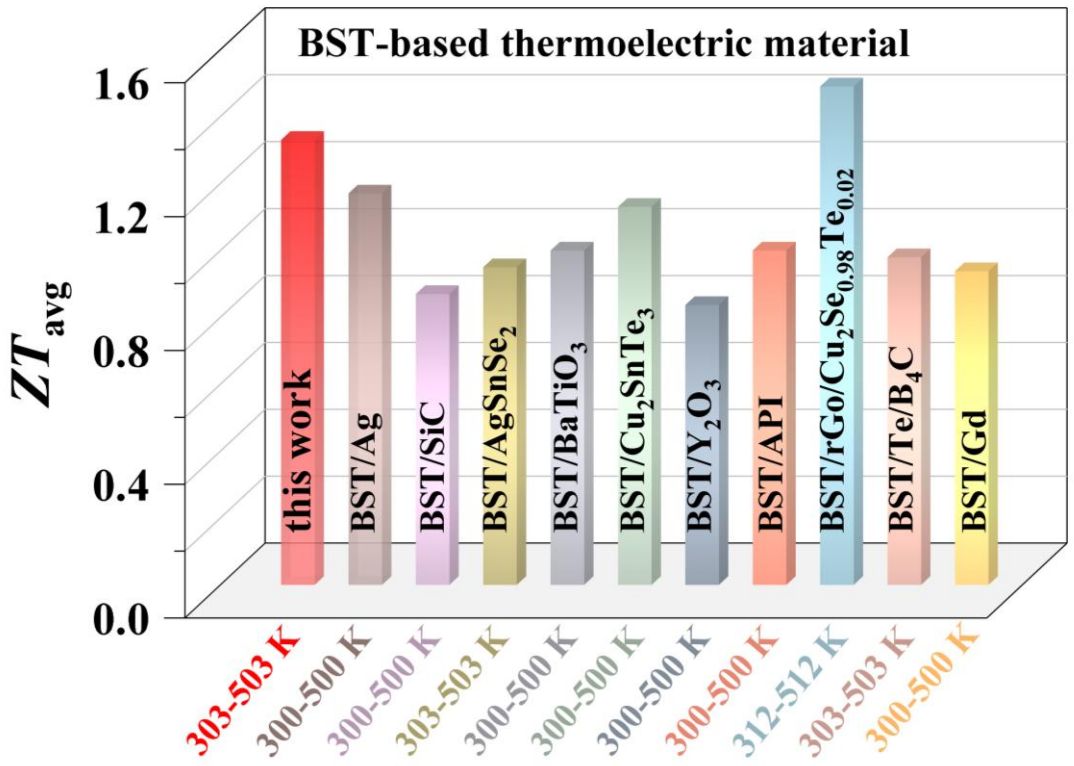

Fig. S13. Compilation of reported average ZT_{avg} over 303-503 K for *p*-type $Bi_{0.5}Sb_{1.5}Te_3$/secondary phase composites from previous studies.[4-13]

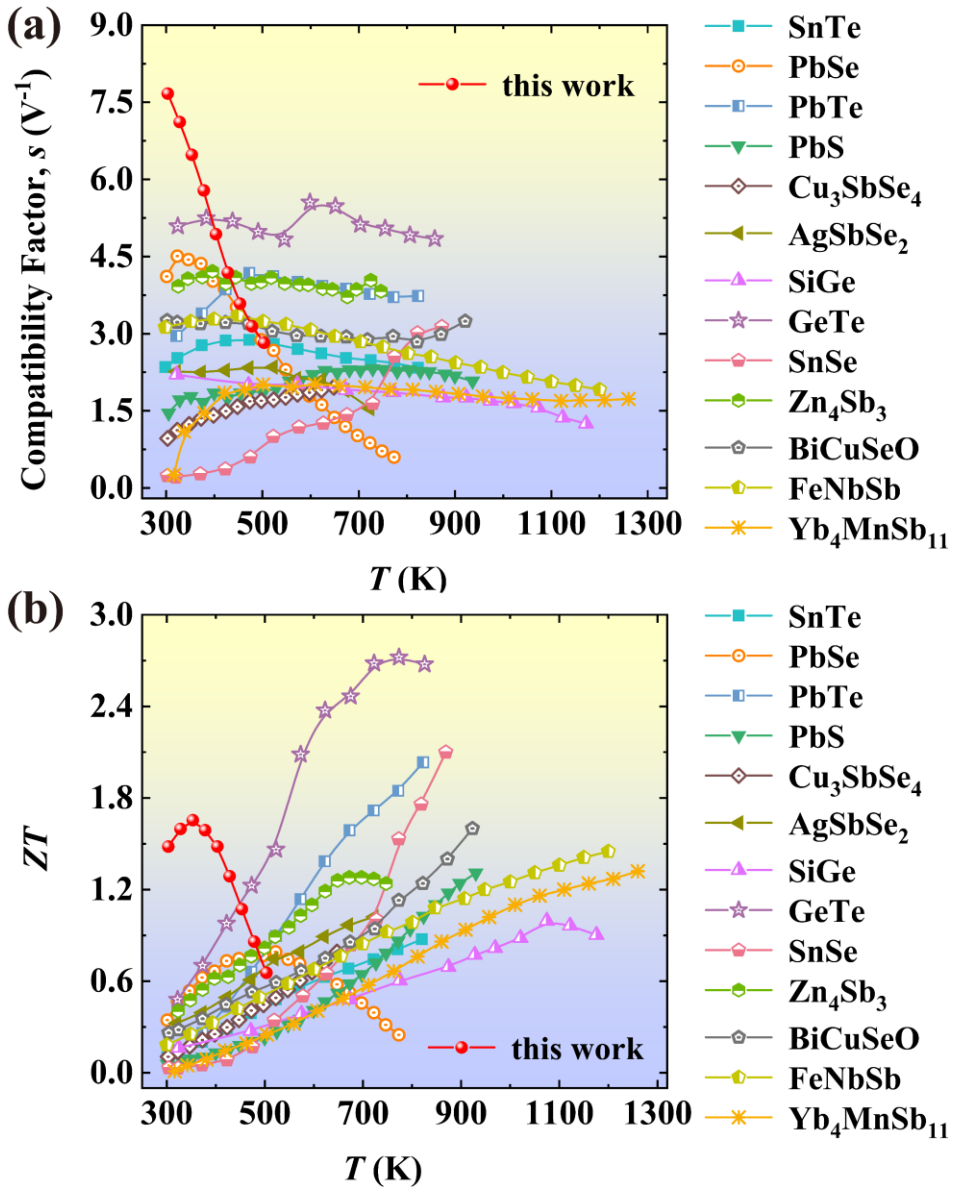

Fig. S14. Temperature dependence of (a) compatibility factor (*s*) and (b) *ZT* for representative *p*-type thermoelectric materials.[20-32]

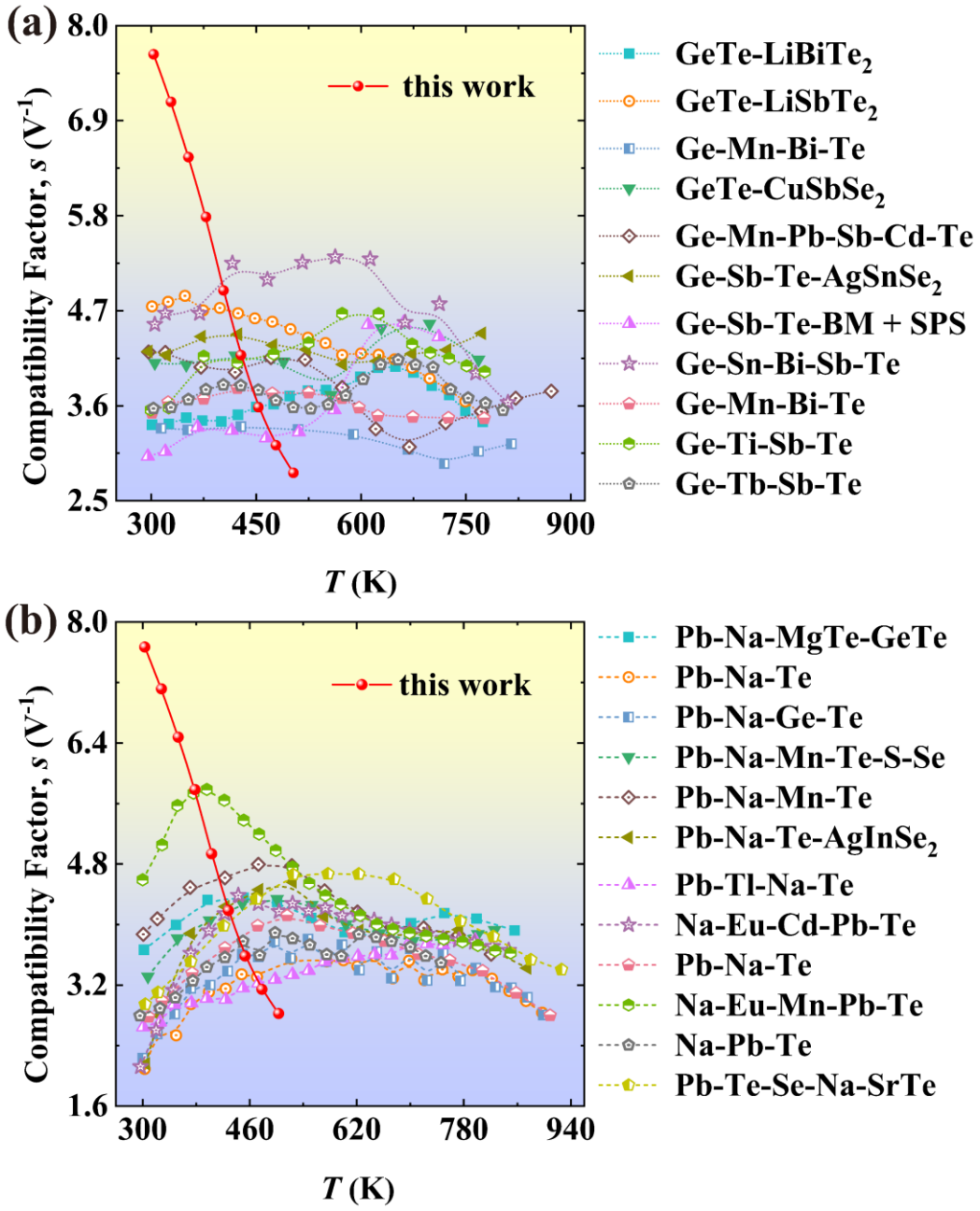

Figure S15. Temperature-dependent compatibility factor of representative high-performance materials: (a) cubic GeTe[33-43] and *p*-type PbTe.[44-54]

References:

1. J. J. Kuo, S. D. Kang, K. Imasato, H. Tamaki, S. Ohno, T. Kanno and G. J. Snyder, *Energy & Environmental Science*, 2018, **11**, 429-434.
2. G. J. Snyder, A. H. Snyder, M. Wood, R. Gurunathan, B. H. Snyder and C. Niu, *Advanced Materials*, 2020, **32**, 2001537.
3. Y. Zhang, K. Pang, Q. Zhang, Y. Li, W. Zhou, X. Tan, J. G. Noudem, G. Wu, L. Chen and H. Hu, *Small Methods*, 2024, **8**, 2301256.
4. W. Xie, B. Zhu, X. Wu, W. Cao and Z. Wang, *Journal of the European Ceramic Society*, 2024, **44**, 5765-5773.
5. Q. Pan, K. Pang, Q. Zhang, Y. Liu, H. Shi, J. Li, W. Zhou, Q. Sun, Y. Zhang, X. Tan, P. Sun, J. Wu, G. Q. Liu and J. Jiang, *Journal of Materials Chemistry A*, 2024, **12**, 8785-8795.
6. B. Zhu, W. Xie, R. Huang, Y. Zheng, W. Cao, Y. Hou and Z. Wang, *Materials Today Energy*, 2024, **46**, 101717.
7. Y. Cheng, J. Yang, Y. Luo, W. Li, A. Vtyurin, Q. Jiang, S. Dunn and H. Yan, *ACS Applied Materials & Interfaces*, 2022, **14**, 37204-37212.
8. B. Zhu, Y. Luo, H. Wu, D. Sun, L. Liu, S. Shu, Z. Z. Luo, Q. Zhang, A. Suwardi and Y. Zheng, *Journal of Materials Chemistry A*, 2023, **11**, 8912-8921.
9. C. C. Li, M. W. Zhang, J. W. Xin, L. Wei and W. Y. Zhao, *Rare Metals*, 2024, **43**, 1758-1768.
10. X. Niu, Y. Lang, L. Pan and Y. Wang, *Journal of Alloys and Compounds*, 2023, **956**, 170399.
11. S. Li, L. Wang, D. Ma, Y. Jiang, J. Zhang and K. Guo, *ACS Applied Materials & Interfaces*, 2024, **16**, 3586-3592.
12. C. Liu, W. Xu, P. Wei, S. Ke, W. Cui, L. Li, D. Liang, X. Ye, T. Chen, X. Nie, W. Zhu, W. Zhao and Q. Zhang, *Energy & Environmental Materials*, 2024, **7**, e12710.
13. R. Chueachot and R. Nakhowong, *Journal of Materiomics*, 2024, **10**, 1091-1100.
14. P. K. Nguyen, K. H. Lee, J. Moon, S. I. Kim, K. A. Ahn, L. H. Chen, S. M. Lee, R. K. Chen, S. Jin and A. E. Berkowitz, *Nanotechnology*, 2012, **23**, 415604.
15. Y. Yu, D. S. He, S. Y. Zhang, O. Cojocaru-Mirédin, T. Schwarz, A. Stoffers, X. Y. Wang, S. Q. Zheng, B. Zhu, C. Scheu, D. Wu, J. Q. He, M. Wuttig, Z. Y. Huang and F. Q. Zu, *Nano Energy*, 2017, **37**, 203-213.
16. J. J. Shen, T. J. Zhu, X. B. Zhao, S. N. Zhang, S. H. Yang and Z. Z. Yin, *Energy & Environmental Science*, 2010, **3**, 1519-1523.
17. P. Sharief, B. Madavali, P. Dharmaiah, J. W. Song, S. Gian, Y. Sohn, J. H. Han, S. H. Song and S. J.

Hong, *Journal of the European Ceramic Society*, 2022, **42**, 3473-3479.

18. J. Qiu, T. Luo, Y. Yan, F. Xia, L. Yao, X. Tan, D. Yang, G. Tan, X. Su, J. Wu and X. Tang, *ACS Applied Materials & Interfaces*, 2021, **13**, 58974-58981.
19. D. Shin, P. Dharmaiah, J. W. Song and S. J. Hong, *Materials*, 2021, **14**, 2993.
20. C. Fu, S. Bai, Y. Liu, Y. Tang, L. Chen, X. Zhao and T. Zhu, *Nature Communications*, 2015, **6**, 8144.
21. T. W. Lan, K. H. Su, C. C. Chang, C. L. Chen, C. L. Chen, M. N. Ou, D. Z. Wu, P. M. Wu, C. Y. Su, M. K. Wu and Y. Y. Chen, *Materials Today Physics*, 2020, **13**, 100215.
22. X. Li, B. Ma, S. Liu, F. Zhang, Y. Li, X. Chao, Z. Yang, J. He and D. Wu, *ACS Applied Energy Materials*, 2022, **6**, 530-536.
23. J. Lin, L. Ma, Q. Liu, K. Xie, Y. Hu, L. Zhang, S. Li, M. Lu and G. Qiao, *Materials Today Energy*, 2021, **21**, 100787.
24. C. Liu, Z. Zhang, Y. Peng, F. Li, L. Miao, E. Nishibori, R. Chetty, X. Bai, R. Si, J. Gao, X, Wang, Y. Zhu, N. Wang, H. Wei and T. Mori, *Science Advances*, 2023, **9**, eadh0713.
25. F. Lv, Y. Zhong, X. Zhao, X. An, Q. Deng, L. Gan, L. Lin and R. Ang, *Small*, 2023, **19**, 2301352.
26. X. Qian, H. R. Guo, J. X. Lyu, B. F. Ding, X. Y. San, X. Zhang, J. L. Wang and S. F. Wang, *Rare Metals*, 2024, **43**, 3232-3241.
27. B. Su, Z. Han, Y. Jiang, H. L. Zhuang, J. Yu, J. Pei, H. Hu, J. W. Li, Y. X. He, B. P. Zhang and J. F. Li, *Advanced Functional Materials*, 2023, **33**, 2301971.
28. E. S. Toberer, C. A. Cox, S. R. Brown, T. Ikeda, A. F. May, S. M. Kauzlarich and G. J. Snyder, *Advanced Functional Materials*, 2008, **18**, 2795-2800.
29. D. Zhang, R. Zhong, S. Gao, L. Yang, F. Xu, P. He, G. Liu, X. San, J. Yang, Y. Luo and S. Wang, *Science China Materials*, 2023, **66**, 3644-3650.
30. L. D. Zhao, J. He, S. Hao, C. I. Wu, T. P. Hogan, C. Wolverton, V. P. Dravid and M. G. Kanatzidis, *Journal of the American Chemical Society*, 2012, **134**, 16327-16336.
31. Z. Zhou, J. Guo, Y. Zheng, Y. Yang, B. Yang, D. Li, W. Zhang, B. Wei, C. Liu, J. L. Lan, C. W. Nan and Y. H. Lin, *Small Methods*, 2024, **8**, 202301619.
32. Y. Zhu, D. Wang, T. Hong, L. Hu, T. Ina, S. Zhan, B. Qin, H. Shi, L. Su, X. Gao and L. D. Zhao, *Nature Communications*, 2022, **13**, 4179.
33. S. Chen, Y. Zhong, J. Cai, Z. Zhang, F. Gao, S. Huo, J. Wu, C. Cui, X. Tan, G. Liu, D. Fang and J. Jiang, *Materials Today Physics*, 2024, **43**, 101393.
34. F. Guo, M. Liu, J. Zhu, Z. Liu, Y. Zhu, M. Guo, X. Dong, Q. Zhang, Y. Zhang, W. Cai and J. Sui, *Materials Today Physics*, 2022, **27**, 100780.
35. M. Li, M. Hong, X. Tang, Q. Sun, W. Y. Lyu, S. D. Xu, L. Z. Kou, M. Dargusch, J. Zou and Z. G.

Chen, *Nano Energy*, 2020, **73**, 104740.

36. G. Liang, T. Lyu, L. Hu, W. Qu, S. Zhi, J. Li, Y. Zhang, J. He, J. Li, F. Liu, C. Zhang, W. Ao, H. Xie and H. Wu, *ACS Applied Materials & Interfaces*, 2021, **13**, 47081-47089.
37. M. Liu, J. Zhu, B. Cui, F. Guo, Z. Liu, Y. Zhu, M. Guo, Y. Sun, Q. Zhang, Y. Zhang, W. Cai and J. Sui, *Cell Reports Physical Science*, 2022, **3**, 100902.
38. Z. H. Liu, J. F. Sun, J. Mao, H. T. Zhu, W. Y. Ren, J. C. Zhou, Z. M. Wang, D. J. Singh, J. H. Sui, C. W. Chu and Z. F. Ren, *Proceedings of the National Academy of Sciences of the United States of America*, 2018, **115**, 5332-5337.
39. N. Man, J. Cai, Z. Guo, G. Liu, P. Sun, H. Wang, Q. Zhang, X. Tan, Y. Yin and J. Jiang, *ACS Applied Energy Materials*, 2021, **4**, 4242-4247.
40. D. Sarkar, M. Samanta, T. Ghosh, K. Dolui, S. Das, K. Saurabh, D. Sanyal and K. Biswas, *Energy & Environmental Science*, 2022, **15**, 4625-4635.
41. A. Suwardi, J. Cao, L. Hu, F. X. Wei, J. Wu, Y. S. Zhao, S. H. Lim, L. Yang, X. Y. Tan, S. A. W. Chien, Y. Yin, W. X. Zhou, W. L. M. Nancy, X. Z. Wang, S. O. Lim, X. P. Ni, D. F. Li, Q. Y. Yan, Y. Zheng, G. Zhang and J. W. Xu, *Journal of Materials Chemistry A*, 2020, **8**, 18880-18890.
42. S. Zhi, J. Li, L. Hu, J. Li, N. Li, H. Wu, F. Liu, C. Zhang, W. Ao, H. Xie, X. Zhao, S. J. Pennycook and T. Zhu, *Advanced Science*, 2021, **8**, 2100220.
43. F. Xu, B. Liu and R. Ang, *Acta Materialia*, 2025, **296**, 121266.
44. X. An, B. Tian, Q. Deng, H. Ma, W. Yuan, Z. He, R. Li, X. Tan, Q. Sun, R. Ang and Interfaces, *ACS Applied Materials*, 2024, **16**, 4827-4835.
45. B. Cai, J. Li, H. Sun, L. Zhang, B. Xu, W. Hu, D. Yu, J. He, Z. Zhao, Z. Liu and Y. Tian, *Science China Materials*, 2018, **61**, 1218-1224.
46. B. Jia, D. Wu, L. Xie, W. Wang, T. Yu, S. Li, Y. Wang, Y. Xu, B. Jiang , Z. Chen, Y. Weng and J. He, *Science*, 2024, **384**, 81-86.
47. P. Jood, J. P. Male, S. Anand, Y. Matsushita, Y. Takagiwa, M. G. Kanatzidis, G. J. Snyder and M. Ohta, *Journal of the American Chemical Society*, 2020, **142**, 15464-15475.
48. P. Jood, M. Ohta, A. Yamamoto and M. Kanatzidis, *Joule*, 2018, **2**, 1339-1355.
49. T. Parashchuk, B. Wiendlocha, O. Cherniushok, R. Knura. and K. Wojciechowski, *ACS Applied Materials*, 2021, **13**, 49027-49042.
50. Y. Pei, G. Tan, D. Feng, L. Zheng, Q. Tan, X. Xie, S. Gong, Y. Chen, J. F. Li and J. He, *Advanced Energy Materials*, 2017, **7**, 1601450.
51. Y. Wu, P. Nan, Z. Chen, Z. Zeng, R. Liu, H. Dong, L. Xie, Y. Xiao, Z. Chen and H. Gu, *Advanced Science*, 2020, **7**, 1902628.

52. Y. X. Wu, P. F. Nan, Z. W. Chen, Z. Z. Zeng, S. Q. Lin, X. Y. Zhang, H. L. Dong, Z. Q. Chen, H. K. Gu, W. Li, Y. Chen, B. H. Ge and Y. Z. Pei, *Research*, 2020, **2020**, UNSP 8151059.
53. M. Zhang, J. Cai, F. Gao, Z. Zhang, M. Li, Z. Chen, Y. Wang, D. Hu, X. Tan, G. Liu, S. Yue and J. Jun, *ACS Applied Materials*, 2023, **16**, 907-914.
54. Y. Zhu, L. Hu, S. Zhan, T. Ina, X. Gao, T. Hong and L. D. Zhao, *Energy Environmental Science*, 2022, **15**, 3958-3967.